Effects of Bottom Injection on Heat Transfer and Fluid Flow in Rectangular Cavities

Mingking K. Chyu*
Carnegie Mellon University, Pittsburgh, Pennsylvania 15213
and
Stephen G. Schwarz†
Tulane University, New Orleans, Louisiana 70118

A numerical study is performed for investigating the effects of bottom injection on the heat transfer in a cavity. The Reynolds number (based on the cavity height and bulk mean velocity over the cavity) ranges in value from 100 to 1000. The cavity aspect ratios W/D investigated are 1, 6, and 10. The injection flow rate varies between 2–20% of the bulk flow rate. With the injectant temperature maintained the same as the cavity wall temperature, the effects of injection-reduced cavity heat transfer are strongly dependent on all the parameters aforementioned. For given injection rate and Reynolds number, the degree of heat-transfer reduction increases with a decrease of cavity aspect ratio. In addition, the current results suggest that the heat-transfer correlations presented in previous studies for cavities with aspect ratio of unity overestimate the extent of heat-transfer reduction for wider cavities.

Nomenclature

C = fluid specific heat
D = cavity depth or duct height, see Fig. 1
h = local heat-transfer coefficient
k = fluid thermal conductivity
m = ratio of injection flow rate to the mean flow rate at the channel inlet
Nu = Nusselt number, hD/k
Nu_0 = cavity Nusselt number without injection
n = unit vector of transport direction
P = dimensionless pressure, $(p-p_i)/\rho u_i^2$
Pr = fluid Prandtl number, $\mu C/k$
p = pressure
p_i = pressure at inlet of computational domain
q = heat flux
Re = Reynolds number, $\rho u_i D/\mu$
Re_w = Reynolds number based on cavity width, $\rho u_i W/\mu$
T = temperature
T_i = temperature at the inlet of computational domain
T_w = temperature on the solid wall
U = dimensionless velocity in X direction, u/u_i
u = velocity in x direction
u_i = velocity at the inlet of computational domain
V = dimensionless velocity in Y direction, v/u_i
v = velocity in y direction
V_j = dimensionless injection velocity, v_j/u_i
v_j = injection velocity
W = cavity width
w_j = injection width, see Fig. 1
X = dimensionless horizontal coordinate, x/D
x = horizontal coordinate, defined in Fig. 1
Y = dimensionless vertical coordinate, y/D
y = vertical coordinate, defined in Fig. 1

Subscripts

Θ = dimensional temperature, $(T-T_w)/(T_i-T_w)$
ρ = fluid density

Superscript

$\bar{}$ = area-averaged mean quantity

Introduction

THIS study concerns the effects of bottom injection on the flowfield and heat transfer in a rectangular cavity, as shown in Fig. 1. Motivation for the study comes from a desire to better understand the convective transport in the vicinity of a cavity which may be present on an ablating surface, either by design or otherwise. For laminar flow, which corresponds to low velocities or small cavities, such phenomena are frequently encountered in lubrication systems and detection of piping leakage. For cooling of a gas turbine blade, discrete-hole injection often exists near the grooved tip to decrease the tip-leakage flow and alleviate the thermal load in the region. The flow for turbine blade tip application is primarily turbulent and dominated by the forced convection. In addition, under certain circumstances, the rotation and buoyancy effects may be important.

Heat transfer with flow-over cavities, without bottom injection, has been extensively studied for more than three decades. The flowfield over a cavity is characterized by flow separation and shear-layer reattachment resulting in complex flow patterns with substantial effects on the friction drag and heat transfer. Most earlier studies[1,2] relied on flow visualization techniques and thermal measurements to obtain momentum and heat-transfer information in a cavity. Average heat-transfer data were correlated in terms of Nusselt number (Nu) as a function of the Reynolds number (Re) and the cavity aspect ratio (W/D). Several researchers have studied cavity flow and heat transfer using numerical methods to solve the governing elliptic equations.[3,4] Recently, Chyu and his colleagues[5-7] using an analogous mass-transfer method, have examined local heat-transfer distributions over a wide range of cavity aspect ratio and flow conditions. According to these studies, the local heat-transfer coefficient varies significantly over different surfaces and is strongly dependent on the cavity geometry and upstream conditions.

Very limited information on cavity heat transfer with fluid

Presented as Paper 89-0427 at the AIAA 27th Aerospace Sciences Meeting, Reno, NV, Jan. 9-12, 1989; received Feb. 10, 1989; revision received Nov. 6, 1989.

*Associate Professor, Department of Mechanical Engineering. Member AIAA.
†Assistant Professor, Department of Mechanical Engineering. Member AIAA.

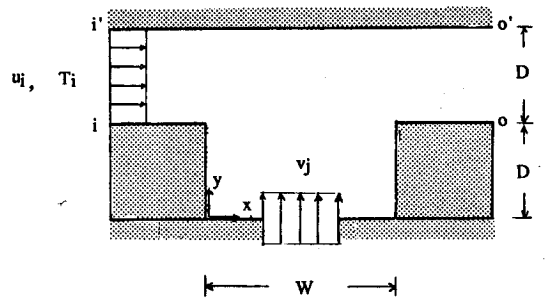

Fig. 1 Rectangular cavity with bottom injection.

injection has been reported to date, and all the published work has dealt exclusively with transpiration-type injection over the entire span of the cavity bottom surface. Chapman,[8] in his pioneer work, analytically predicted that the injection will result in a reduction of the overall heat transfer in the cavity. The ratio of overall heat transfer between the cases, with injection and without, decreases with the injection velocity and Reynolds number. Chapman's analysis assumes that the overall cavity heat transfer is solely determined by the mixing of the separated shear layer; the effects of flow recirculation and recompression are not considered. Johnson and Dhanak,[9] based on their experimental data, later reported similar trends to that of Chapman's analysis. However, the details between these two results are quite different. The experiments performed by Johnson and Dhanak[9] were only limited to cavities having aspect ratio of unity.

In reality, the thermal energy transport in a cavity with injection is often referred to as the so-called "three-temperature" problem. Namely, the thermal-boundary condition in the domain of interest is described by different temperatures of bulk flow, cavity wall, and injection. Such an arrangement is apparently more complex than the conventional, "two-temperature" convection system. The present study, similar to those reported previously,[8,9] assumes the injection temperature maintained the same as that prescribed at the cavity wall. This, to a great extent, alleviates the degree of complexity for analysis, and the influence of injection on the cavity heat transfer becomes primarily hydrodynamic.

In the present study, forced-convection heat transfer for the laminar airflow over a two-dimensional, rectangular cavity with bottom injection from a discrete hole (slot) is numerically investigated. A systematic study is made for different cavity aspect ratios, Reynolds numbers, and injection conditions. The parameters used to describe the injection include the flow rate, width, and location of the injection. Results obtained from this numerical modeling provide detailed information for both local and overall heat-transfer phenomena.

Numerical Computation

The forced flow past a cavity is assumed to be two dimensional, steady, and laminar. The fluid properties are considered to be constant. The governing equations are nondimensionalized using the following definitions of the dimensionless variables:

$$X = x/D, \qquad Y = y/D$$

$$U = u/u_i, \quad V = v/u_i, \quad V_j = v_j/u_i, \quad P = (p - p_i)/\rho u_i^2$$

$$Re = \rho u_i D/\mu \quad Pr = C/k$$

and

$$\Theta = (T - T_w)/(T_i - T_w) \tag{1}$$

The resulting governing equations are as follows:

Continuity

$$\frac{\partial U}{\partial X} + \frac{\partial U}{\partial Y} = 0 \tag{2}$$

X momentum

$$U\frac{\partial U}{\partial X} + \frac{\partial U}{\partial Y} = -\frac{\partial P}{\partial X} + \left(\frac{1}{Re}\right)\left(\frac{\partial^2 U}{\partial X^2} + \frac{\partial^2 U}{\partial Y^2}\right) \tag{3}$$

Y momentum

$$U\frac{\partial V}{\partial X} + V\frac{\partial U}{\partial Y} = \left(\frac{1}{Re}\right)\left(\frac{\partial^2 V}{\partial X^2} + \frac{\partial^2 V}{\partial Y^2}\right) \tag{4}$$

Energy

$$U\frac{\partial \Theta}{\partial X} + V\frac{\partial \Theta}{\partial Y} = \left(\frac{1}{Pr \cdot Re}\right)\left(\frac{\partial^2 \Theta}{\partial X^2} + \frac{\partial^2 \Theta}{\partial Y^2}\right) \tag{5}$$

The value of Pr equals 0.7, which models the airflow. The solution to Eqs. (2-5) is sought within the region bounded by the solid wall, injection, and the planes i-i' to o-o' as indicated in Fig. 1. The following boundary conditions are specified:

1) On all solid walls

$$U = V = 0$$

$$\Theta = 0$$

on lower bounding wall (including surfaces upstream and downstream of cavity and entire cavity surface)

$$\frac{\partial \Theta}{\partial y} = 0 \tag{6}$$

on upper bounding wall

2) At injection

$$U = 0 \qquad V = V_j, \qquad \text{and} \qquad \Theta = 0 \tag{7}$$

3) At inlet boundary (plane i-i')

$$U = 1 \qquad V = 0, \qquad P = 0 \qquad \text{and} \qquad \Theta = 1 \tag{8}$$

4) At outlet boundary (plane o-o')

$$\frac{\partial U}{\partial X} = \frac{\partial V}{\partial X} = \frac{\partial \Theta}{\partial X} = 0 \tag{9}$$

The local heat-transfer coefficient h is defined as

$$h = q/(T_w - T_i) \tag{10}$$

where q is the local heat flux expressed by

$$q = -k\frac{\partial T}{\partial n} \tag{11}$$

on solid boundary and

$$q = \rho C v_j T_j - k\frac{\partial T}{\partial y} \tag{12}$$

at injection hole.

The Nusselt number, which is the dimensionless local heat-transfer coefficient, is given by

$$Nu = hD/k \tag{13}$$

The governing equations are solved using the finite-difference method described in detail by Patankar.[10] The computer program uses the SIMPLER (SIMPLE-Revised) algorithm for the velocity-pressure coupling. All the computations are performed on a 40×26 grid. The choice of this grid size, which gives sufficiently accurate data and reasonable computing time, is resulted from an extensive grid-independence study. The grid is nonuniform and denser near solid surfaces and in the separated shear layer where steeper gradients of dependent variables are expected. The convergence criterion is that the percentage change of a variable at any grid should be less than 0.1%. A typical run on a Micro VAX III workstation takes approximately 150 iterative steps with a CPU time of about 2 min for a converged velocity field, and an additional 50 steps are required for the temperature calculation.

Results and Discussion

To validate the present numerical approach, cavity flow and heat transfer without injection are also studied. Figure 2 shows the computed streamline patterns for cavities with different aspect ratios, i.e., $W/D = 1$, 6, 10. The Reynolds number is the same for all three cases, $Re = 100$. Note that the streamline spacing, as drawn in the figure, is not indicative of the local velocity since the difference in stream function value is not the same between all adjacent lines. This is the case for all the streamline figures in this paper. As expected, the flow patterns shown in Fig. 2 are strongly dependent on the cavity geometry. For $W/D = 1$, the separated shear layer skims over the top of the cavity and inside of the cavity is filled completely with a large vortex. A very small and weak recirculation is also found existing at the downstream lower corner. The dividing streamline, which is indicative of the separated shear layer, is initiated at the sharp corner of the upstream wall (backward-facing wall) and reattaches to the upper portion of the cavity downstream wall (forward-facing wall). The location of this reattachment moves downward as W/D increases. For the widest cavity of the present study, i.e., $W/D = 10$, the shear layer reattaches on the cavity bottom at approximately $X/D = 4$. Near the reattachment point, the shear stress reaches a local maximum and so does the heat-transfer coefficient. The cavity with the shear-layer reattachment on the bottom floor is termed to be "open cavity." The "closed cavity" refers to cavities with low aspect ratios, namely $W/D \sim 1$. The cavity is said to be "closed" by the shear layer completely bridging the two side walls.

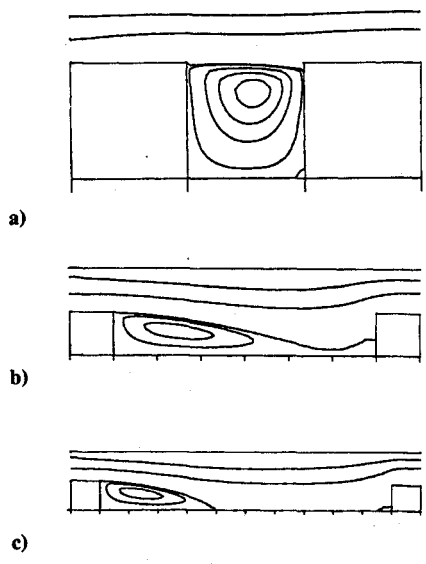

Fig. 2 Cavity flow patterns, without injection: a) $W/D = 1$; b) $W/D = 6$; c) $W/D = 10$.

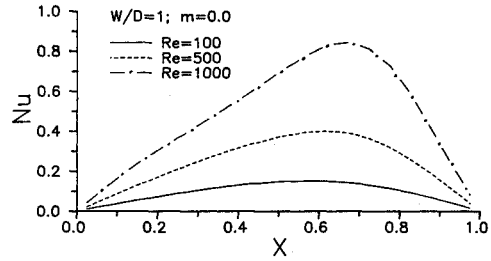

Fig. 3 Local *Nu* on cavity bottom, without injection.

Due to the flow recirculating nature, heat transfer from the surface of a closed cavity is generally low as compared to that with flow in a channel or over a surface without the presence of the cavity. As an example (see Fig. 1), for $W/D = 1$, the entire cavity surface (bottom and two side walls) amounts for 60% of the total heated area in the computational domain, but the heat transfer from the cavity is only about 10%. Among the three surfaces in the cavity, the bottom wall always has the lowest heat transfer, less than one-third of the cavity average. Figure 3 shows the distribution of local Nusselt number on the cavity bottom for $W/D = 1$. The values of *Nu* are very low at the two corners, and a local maximum exists near the midspan. As the Reynolds number increases, the value of this maximum as well as the surface-averaged Nusselt number increases. This general trend agrees well with that reported early by Bhatti and Aung.[3] The actual values of *Nu* of the present study are slightly higher than those reported in Ref. 3; this is considered to be due to the differences in upstream conditions and channel geometry.

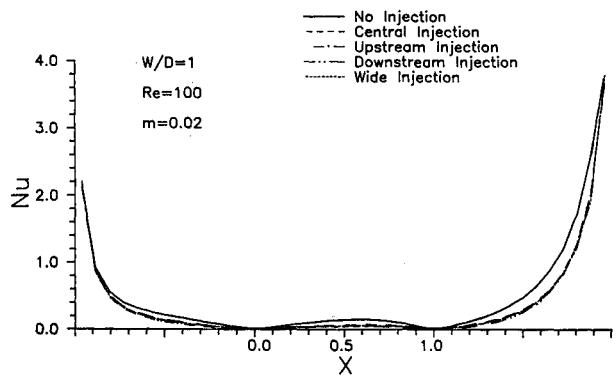

Fig. 4a Effects of injection on cavity local Nusselt number $W/D = 1$; $Re = 100$; $m = 0.02$.

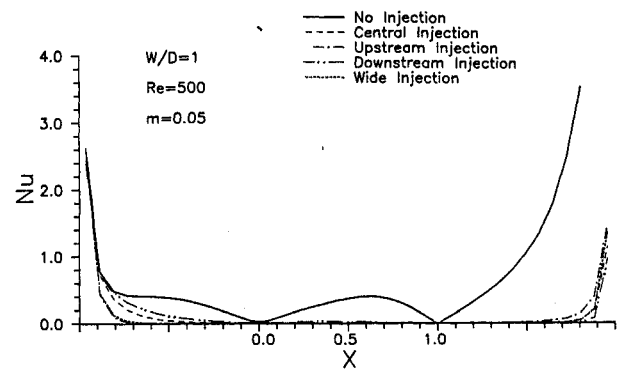

Fig. 4b Effects of injection on cavity local Nusselt number $W/D = 1$; $Re = 500$; $m = 0.05$.

Figure 4 shows the effect of injection on the heat transfer for $W/D=1$. To interpret the figure, it may be helpful to consider the two side walls of the cavity folded out to lie in the plane of the cavity bottom. Upstream, central, and downstream injection refer to the cases for which the center of the injection hole is located at 0.15, 0.5, and 0.85, respectively, of the cavity span. The width of this discrete injection for these three cases is 20% of the cavity width. The wide injection is a central injection with the injection occupying 90% of the cavity width. The wide injection is considered to be similar to the transpiring injection over the entire span of the cavity bottom wall. The parameter m denotes the injection flow rate relative to that of the bulk mean flow. For $Re=100$, $m=0.02$, the injection causes approximately a 30% decrease in the overall cavity heat transfer. Nevertheless, the decrease in the bottom surface is more significant, about 70%. The location as well as the width of injection virtually has no influence on the heat-transfer characteristics of the cavity. However, this trend changes as the Reynolds number and injection rate increase. For the case $Re=500$ with 5% injection, a large portion of the cavity surface experiences extremely low heat-transfer coefficient. Heat transfer from the side walls is sensitive to the location of the injection; the closer the injection, the lower the heat-transfer coefficient. The overall heat-transfer reduction in this case is over 80%.

Figures 5 and 6 display the corresponding streamline patterns for all cases shown in Fig. 4. For $Re=100$, $m=0.02$, flow in the cavity preserves a certain degree of the flow nature without injection. The injectant, when out of the injection hole, follows the local recirculating direction of the large vortex existing in the case without injection. A major vortex still remains but is shifted toward the upper right corner. At a higher Reynolds number, these features change drastically as

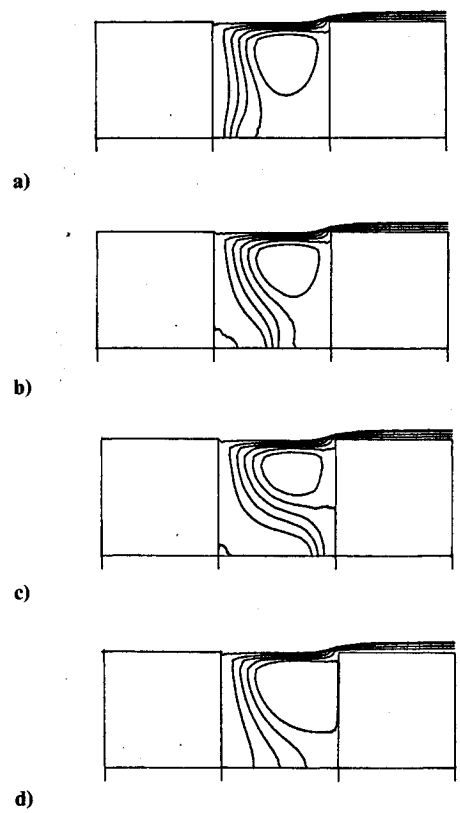

Fig. 5 Cavity flow with injection, $W/D=1$, $Re=100$, $m=0.02$: a) upstream injection; b) central injection; c) downstream injection; d) wide injection.

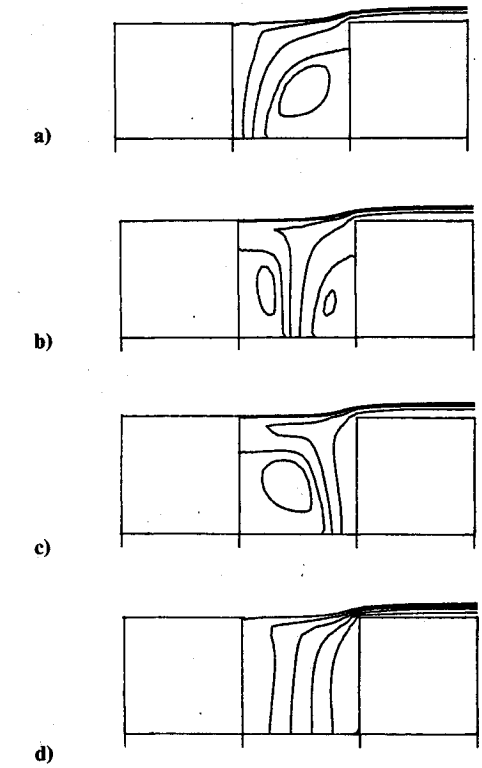

Fig. 6 Cavity flow pattern with injection, $W/D=1$, $Re=500$, $m=0.05$: a) upstream injection; b) central injection; c) downstream injection; d) wide injection.

seen in Fig. 6. Flow near the bottom surface or the lower portion of the cavity is dominated by the injection. As the injection loses its momentum towards the upper portion of the cavity, the shear in the separated layer resumes its influence on the flow. Under this condition, the large vortex existing in the noninjection case is no longer observed. However, there are secondary vortices in the vicinity of injection for the discrete injection. The wide injection results in a vortex-free flowfield.

Figures 7 and 8 show the injection effects on the cavity heat transfer for $W/D=6$ and 10, respectively. In both cases, the influence of injection location is much greater as compared to the case of $W/D=1$. Except for wide injection, the injection appears to be a "regional phenomenon"—only the immediate vicinity or downstream of the injection is affected. As a result, the downstream injection has virtually no effect on the heat transfer in a large portion of the cavity. In terms of the reduction of the heat transfer from the cavity bottom, the upstream or the wide injection is the most effective. In fact, the overall

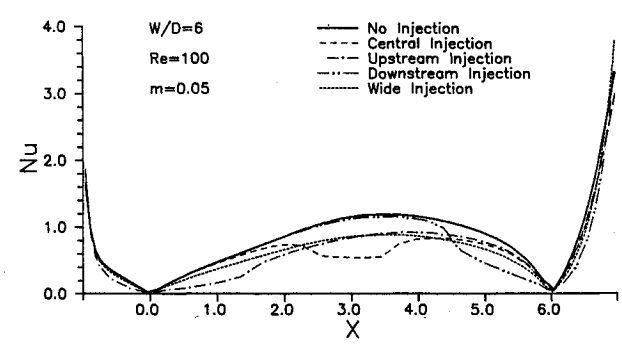

Fig. 7 Effects of injection on cavity local Nusselt number, $W/D=6$, $Re=100$.

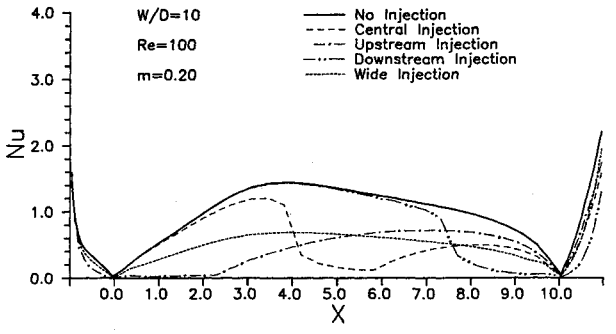

Fig. 8 Effects of injection on cavity local Nusselt number, $W/D=10$, $Re=100$.

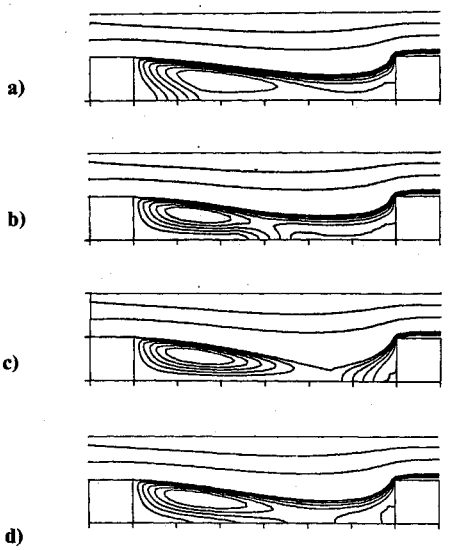

Fig. 9 Cavity flow with injection, $W/D=6$, $Re=100$, $m=0.05$: a) upstream injection; b) central injection; c) downstream injection; d) wide injection.

reduction of heat transfer between these two injection modes are very comparable. Figure 9 illustrates the computed streamlines corresponding to the cases shown in Fig. 7. Even with a 5% injection rate, the injectant follows the general direction of the flow pattern without injection. Comparing this with the case of $W/D=1$ reveals that, to reach the same level of heat-transfer reduction, an open cavity requires a higher injection rate than a closed cavity. An interesting observation is that, for cases with central injection and wide injection, the injecting fluids break into two parts—one flowing in the upstream and the other in the downstream direction. The same phenomenon also occurs for $W/D=10$. Such a flow division is most significantly observed when the injection is near the reattachment point.

Of particular interest is the effect of injection on the overall heat transfer from the cavity. As mentioned previously, all the earlier studies are concerned with transpiring injection. According to an analysis by Chapman,[8] the reduction of heat transfer, which could be expressed in terms of $\overline{Nu}/\overline{Nu}_0$, is a decreasing function of $V_j Re_w^{0.5}$, where $\overline{Nu}_0$ is the area-averaged Nusselt number without injection, and Re_w is the Reynolds number based on cavity width. His analysis assumes that the mixing in the separated shear layer is the sole factor determining the heat transfer in the cavity. Based on the empirical data for $W/D=1$, Johnson and Dhanak[9] proposed that $\overline{Nu}/\overline{Nu}_0$ is proportional to $\exp(-0.43\ V_j Re_w^{0.77})$. The present computational results in wide injection, together with

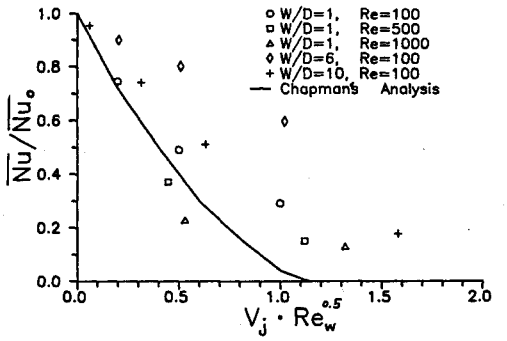

Fig. 10 Effects of injection on cavity overall heat transfer—comparison with Chapman's analysis.

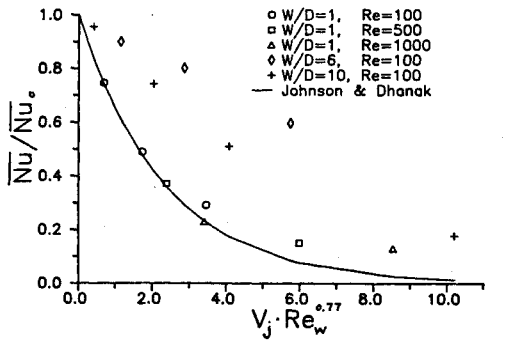

Fig. 11 Effects of injection on cavity overall heat transfer—comparison with Johnson and Dhanak results.

each of these two correlations, are presented in Figs. 10 and 11, respectively. Examining these two figures reveals that both correlations greatly overestimate the injection effect for the open cavities. The simple model assumed in Chapman's analysis appears to be insufficient for the open cavities, as expected. In addition, the Johnson and Dhanak correlation only prevails within its testing range, i.e., $W/D=1$. This is evidenced by an excellent agreement for low Reynolds number and low injection rate, as shown in Fig. 11.

Concluding Remarks

Cavity flow and heat transfer with emphasis on the fluid injection from the cavity bottom are numerically investigated. As a reference, the computed flowfields and heat transfer in cavities without injection agree well with those reported earlier in the literature. The injection generally reduces the heat transfer from cavity, and the degree of reduction is strongly aspect-ratio dependent. With the same injection rate and Reynolds number, a closed cavity has a stronger overall heat-transfer reduction than an open cavity. Thus earlier correlations based on simple mixing model or closed-cavity data are insufficient to describe the injection effects for the open cavity. In addition, for a given injection rate, the heat transfer in a closed cavity is insensitive to the location and the width of the injection. The opposite trend is observed for the open cavity.

References

[1]Haugen, R. L., and Dhanak, A. M., "Heat Transfer in Turbulent Boundary Layer Separation Over a Surface Cavity," *Journal of Heat Transfer,* Vol. 89, Nov. 1967, pp. 335-340.

[2]Yamamoto, H., Seki, N., and Fukusako, S., "Forced Convection Heat Transfer on Bottom Surface of a Cavity," *Journal of Heat Transfer,* Vol. 101, Aug. 1979, pp. 475-479.

[3]Bhatti, A., and Aung, W., "Finite Difference Analysis of Laminar Separated Forced Convection in Cavities," *Journal of Heat Transfer,*

Vol. 106, Feb. 1984, pp. 49–54.
[4]Chyu, M. K., Metzger, D. E., and Hwan, C. L., "Heat Transfer in Shrouded Rectangular Cavities, *Journal of Thermophysics and Heat Transfer,* Vol. 1, July 1987, pp. 247–252.
[5]Chyu, M. K., and Goldstein, R. J., "Local Mass Transfer in Rectangular Cavities with Separated Turbulent Flow," *Heat Transfer 1986,* Vol. 3, Hemisphere, Washington, DC, 1986, pp. 1065–1070.
[6]Chyu, M. K., Moon, H. K., and Metzger, D. E., "Heat Transfer in the Tip Region of Grooved Turbine Blades," *Journal of Turbomachinery,* Vol. 111, April 1989, pp. 131–138.
[7]Chyu, M. K., and Kapat, J. S., "Local Mass Transfer in Skewed Rectangular Cavities," *Transport Phenomena in Turbulent Flows,* Hemisphere, Washington, DC, 1988, pp. 515–530.
[8]Chapman, D. R., "A Theoretical Analysis of Heat Transfer in Regions of Separated Flow," NACA TN-3792, 1956.
[9]Johnson, R. W., and Dhanak, A. M., "Heat Transfer in Laminar Flow Past a Rectangular Cavity with Fluid Injection," *Journal of Heat Transfer,* Vol. 98, May 1976, pp. 226–231.
[10]Patankar, S. V., *Numerical Heat Transfer and Fluid Flow,* McGraw Hill, New York, 1980.